

# Improving the exchange and correlation potential in density functional approximations through constraints

Timothy J. Callow,<sup>1,2,\*</sup> Benjamin J. Pearce,<sup>1,†</sup> Tom Pitts,<sup>1,‡</sup> Nektarios N. Lathiotakis,<sup>3,§</sup> Matthew J.P. Hodgson,<sup>1,¶</sup> and Nikitas I. Gidopoulos<sup>1,\*\*</sup>

<sup>1</sup>*Department of Physics, Durham University,  
South Road, Durham, DH1 3LE, United Kingdom*

<sup>2</sup>*Max-Planck-Institut für Mikrostrukturphysik,  
Weinberg 2, D-06120 Halle, Germany*

<sup>3</sup>*Theoretical and Physical Chemistry Institute,  
National Hellenic Research Foundation,  
Vass. Constantinou 48, 116 35 Athens, Greece*

(Dated: July 31, 2022)

We review and expand on our work to impose constraints on the effective Kohn Sham (KS) potential of local and semi-local density functional approximations. In this work, we relax a previously imposed positivity constraint, which increased the computational cost and we find that it is safe to do so, except in systems with very few electrons. The constrained minimisation leads invariably to the solution of an optimised effective potential (OEP) equation in order to determine the KS potential. We review briefly our previous work on this problem and demonstrate with numerous examples that despite well-known mathematical issues of the OEP with finite basis sets, our OEP equations are well behaved. We demonstrate that constraining the screening charge of the Hartree, exchange and correlation potential not only corrects its asymptotic behaviour but also allows the exchange and correlation potential to exhibit nonzero derivative discontinuity, a feature of the exact KS potential that is necessary for the accurate prediction of band-gaps in solids but very hard to capture with semi-local approximations.

## I. INTRODUCTION

A challenge with common density functional approximations is the imbalance of accuracy between the energy functionals and the corresponding Kohn-Sham (KS) potentials, i.e. the functional derivatives of the energy density-functionals. Although the accuracy and quality of an energy density-functional is often quite good, the resulting KS potential is inferior [1–3]. The quest to come up with ever more accurate energy density-functionals to obtain moderate improvements on the KS potential may not be the best strategy (diminishing returns in the accuracy of the KS potential) and we explore different routes to improved accuracy of the calculation.

A way we explored to improve the quality of the KS potential was to define appropriate potential-functionals of an energy difference, instead of density-functionals of the total energy, and to minimise the aforementioned energy difference rather than the total energy [4, 5, 7, 28]. The advantage of the approach is that the energy difference is bound from below, even in approximations from finite-order (second) perturbation theory; the latter can then be employed directly to derive accurate XC potentials without the risk of variational collapse [4, 7].

In this paper, we review briefly and expand on our work [8–10] to improve the performance of local and semi-local density-functional approximations (DFAs), by imposing physical constraints on the single-particle, local, effective (KS) potential, whose orbitals minimise the total energy functional. In Refs. 8–10 we argued that these constraints improve the asymptotic behaviour and overall quality of the KS potential by removing the erroneous effects of self-interactions (SIs) from it. As evidence, we demonstrated that, compared with the results from the unconstrained minimisation, the ionisation potentials (IPs) [35] of a large number of atoms, molecules, even anions, obtained from our constrained minimisation improved significantly, while the calculated total energies increased only minimally.

In this work, we further show that with a judicious choice, the constraints imposed on

---

\*Electronic address: timothy.callow@durham.ac.uk

†Electronic address: b.j.pearce@durham.ac.uk

‡Electronic address: tom.pitts@durham.ac.uk

§Electronic address: lathiot@eie.gr

¶Electronic address: matthew.j.hodgson@durham.ac.uk

\*\*Electronic address: nikitas.gidopoulos@durham.ac.uk

the KS potential of local and semi-local DFAs enable their (constrained) exchange and correlation (xc) potential to exhibit exotic, non-analytic behaviour, expected only in more elaborate and computationally costly levels of theory, or from higher, heavenly rungs on Jacob's ladder of DFAs, as envisaged by John Perdew and co-workers [12].

## II. CONSTRAINED MINIMISATION OF DENSITY FUNCTIONAL APPROXIMATIONS

In the constrained minimisation method [8–10], the Hxc screening density, or electron repulsion density,  $\rho_{scr}^{DFA}(\mathbf{r})$ , defined via Poisson's equation [15–17],

$$\nabla^2 v_{Hxc}^{DFA}(\mathbf{r}) = -4\pi\rho_{scr}^{DFA}(\mathbf{r}), \quad (1)$$

plays an equally important role as the Hxc potential. For example, the integrated screening charge,

$$Q_{scr} \doteq \int d^3r \rho_{scr}(\mathbf{r}), \quad (2)$$

of the exact KS potential satisfies the intuitive sum rule,  $Q_{scr} = N - 1$  [15–17]. In Ref. 8, we argued that the violation of the sum rule in LDA and most GGAs (where  $Q_{scr}^{DFA} = N$ ), can be attributed to SIs, since it implies that any one of the electrons of an  $N$  electron system is effectively repelled, via the Hxc potential, by a net charge of  $N$  electrons.

Accordingly, in the constrained minimisation of DFAs [8–10], our strategy to mitigate the effects of SIs from the effective potential is to set that the KS orbitals satisfy single-particle equations,

$$\left[ -\frac{\nabla^2}{2} + v_{en}(\mathbf{r}) + v(\mathbf{r}) \right] \phi_i(\mathbf{r}) = \epsilon_i \phi_i(\mathbf{r}) \quad (3)$$

with the Hxc potential replaced by the screening, or electron repulsion potential,  $v(\mathbf{r})$ ,

$$v(\mathbf{r}) = \int d^3r' \frac{\rho_{scr}(\mathbf{r}')}{|\mathbf{r} - \mathbf{r}'|}, \quad (4)$$

where  $\rho_{scr}(\mathbf{r})$  satisfies two constraints:

$$Q_{scr} = N - 1, \quad (5)$$

and

$$\rho_{scr}(\mathbf{r}) \geq 0. \quad (6)$$

The second constraint (6) is physically intuitive, hinting at interpreting  $\rho_{scr}(\mathbf{r})$  as the charge density of  $N-1$  electrons. However, the positivity condition (6) is too strong and not satisfied by the exact KS potential.

The positivity constraint (6) has a double role in the constrained minimisation method. Primarily, it allows the mathematical problem of constrained minimisation to remain well posed in the limit of complete orbital and auxiliary basis sets [8, 9]. Secondly, with finite orbital and auxiliary basis sets, the positivity constraint (6) offers a simple way to reduce drastically the variational flexibility of  $\rho_{scr}(\mathbf{r})$  and of  $v(\mathbf{r})$  and thereby helps to overcome mathematical pathologies [19] in the solution of the optimised effective potential (OEP) equation [13, 14]. These pathologies have hindered the wider application of the OEP method; see our analysis in Ref. 20 and the discussion in Refs. 21, 22.

Following Ref. 20, the indeterminacy of the OEP with finite basis sets can be overcome efficiently by extending the domain of the response function. We review the main idea below.

The density-density response function is given, for  $\lambda = 1$ , by

$$\chi_v^\lambda(\mathbf{r}, \mathbf{r}') = \chi_v^0(\mathbf{r}, \mathbf{r}') + \lambda \bar{\chi}_v(\mathbf{r}, \mathbf{r}'), \quad (7)$$

with

$$\chi_v^0(\mathbf{r}, \mathbf{r}') = \sum_i^{\text{occ}} \sum_{a \in \text{OB}}^{\text{unocc}} \frac{\phi_i(\mathbf{r}) \phi_a^*(\mathbf{r}) \phi_i^*(\mathbf{r}') \phi_a(\mathbf{r}')}{\epsilon_i - \epsilon_a} + \text{c.c.} \quad (8)$$

$$\bar{\chi}_v(\mathbf{r}, \mathbf{r}') = \sum_i^{\text{occ}} \sum_{b \notin \text{OB}}^{\text{unocc}} \frac{\phi_i(\mathbf{r}) \phi_b^*(\mathbf{r}) \phi_i^*(\mathbf{r}') \phi_b(\mathbf{r}')}{\epsilon_i - \epsilon_b} + \text{c.c.} \quad (9)$$

The sum is over occupied  $\{\phi_i\}$  and unoccupied  $\{\phi_a, \phi_b\}$  KS orbitals (3) in the KS Slater determinant. We take for simplicity that the orbital basis set (OB) is composed exactly of a set of low lying KS orbitals,  $\text{OB} = \{\phi_i\} \cup \{\phi_a\}$ , i.e., the set of orbitals which are occupied in the KS state and the lowest unoccupied ones. Until Ref. 20, when working with finite orbital basis sets, the complement  $\bar{\chi}_v$  of the response function was typically omitted.

We are interested in the limit of  $\chi_v^\lambda$  for small  $\lambda$ . Using the Unsöld approximation [23], the complement of the response function  $\bar{\chi}_v$  reduces to

$$\bar{\chi}_v(\mathbf{r}, \mathbf{r}') \simeq \frac{2\rho(\mathbf{r}, \mathbf{r}') \rho(\mathbf{r}', \mathbf{r}) - \delta(\mathbf{r} - \mathbf{r}') \rho(\mathbf{r}, \mathbf{r}') - \delta(\mathbf{r} - \mathbf{r}') \rho(\mathbf{r}', \mathbf{r})}{\Delta} \quad (10)$$

where  $-\Delta$  is the common energy denominator that replaces  $\epsilon_i - \epsilon_b$  in (9),  $\Delta > 0$ .

$\rho(\mathbf{r}, \mathbf{r}')$  is the single-particle density matrix of the occupied orbitals

$$\rho(\mathbf{r}, \mathbf{r}') = \sum_i^{\text{occ}} \phi_i(\mathbf{r}) \phi_i^*(\mathbf{r}'). \quad (11)$$

In (10), we omit a term with the same domain as  $\chi_v^0$ , because its contribution to  $\chi_v^\lambda$  vanishes for small  $\lambda$ .

We shall see that, as long as  $\Delta > 0$ , the value of  $\Delta$  does not play a role in the results, since  $\Delta$  always appears together with  $\lambda$ , in the ratio  $\lambda/\Delta$ , and we investigate the limit  $\lambda \rightarrow 0$ . In the end, we shall also consider the limit  $\lambda \rightarrow \infty$ , for which the value of positive  $\Delta$  does not matter either.

It is straightforward to confirm that  $\bar{\chi}_v$  is negative semi-definite, like  $\chi_v^0$ , and that the only null eigenfunction of  $\bar{\chi}_v$  is the constant function.

A typical OEP equation has the form

$$[\chi_v^0(\mathbf{r}, \mathbf{r}') + \lambda \bar{\chi}_v(\mathbf{r}, \mathbf{r}')] v^\lambda(\mathbf{r}) = b^0(\mathbf{r}) + \lambda \bar{b}(\mathbf{r}) \quad (12)$$

where the evaluation of  $\bar{b}(\mathbf{r})$  on the r.h.s., for a finite orbital basis, involves the Unsöld approximation [23].

Prior to Ref. 20, the finite orbital basis OEP was given by the solution of (12) at  $\lambda = 0$ . However, this solution leaves the effective potential  $v^0(\mathbf{r})$  indeterminate in the null space of  $\chi_v^0$ , which is infinite-dimensional. In order to obtain a smooth potential,  $v^0(\mathbf{r})$ , one must restrict the freedom of  $v^0(\mathbf{r})$ , e.g. by expanding in a properly chosen auxiliary basis and then increase the size of the orbital basis, at increasing computational cost, until the domain of  $\chi_v^0$  covers the auxiliary space.

The main point of Ref. 20 is the observation that the solution of the same equation (12) for any finite  $\lambda > 0$ , even  $\lambda$  tending to zero, determines the effective potential fully, up to a constant. The extension of the response function with  $\bar{\chi}_v$  amounts to using an effectively complete orbital basis. We note that the solution of (12) is smooth for any  $\lambda > 0$ , including the limits for small and for large  $\lambda$ , which correspond respectively to the OEP potential in a finite orbital basis,  $v^{\lambda \rightarrow 0}(\mathbf{r})$ , and to its (Unsöld) approximation with a common energy denominator,  $v^\infty(\mathbf{r})$ . It turns out that for the effective xc potentials in the constrained minimisation method, the two solutions are close to each other.

### A. Relaxing the positivity constraint

In Refs. 8–10 we solved the OEP equation for the CLDA and CDFA method, using finite orbital and auxiliary basis sets, with  $\lambda = 0$ . The indeterminacy of the effective potential

was restricted by expressing  $v(\mathbf{r})$  in terms of the screening density  $\rho_{scr}(\mathbf{r})$  in (4) and then constraining the screening charge  $Q_{scr}$  (5) as well as the sign of  $\rho_{scr}(\mathbf{r})$  (6).

However, the positivity constraint, implemented with a penalty function [10] is a computational bottleneck for the calculation. In a forthcoming paper, we implement the positivity constraint more efficiently, by writing  $\rho_{scr}(\mathbf{r}) = |f_{scr}(\mathbf{r})|^2$ , and solving for the screening amplitude  $f_{scr}(\mathbf{r})$  [24].

In the next part, we investigate the effects of relaxing the positivity constraint on the convergence of the screening potential and screening density. A weak effect, for sufficiently flexible auxiliary basis sets, will justify the relaxation of the positivity constraint and reduce the computation effort. The auxiliary basis sets we use are un-contracted cc-pVXZ [30, 34], with X=D,T,Q.

In the rest of the section, we show indicative results of CLDA, where the minimisation was performed under just the constraint for the screening charge,  $Q_{scr} = N - 1$  (5). In order to determine  $v(\mathbf{r})$  and  $\rho_{scr}(\mathbf{r})$ , we employ the extended response function  $\chi_v^\lambda(\mathbf{r}, \mathbf{r}')$ , in the limit of small  $\lambda$ . We use  $\lambda/\Delta = 0.01$ , but the results seem converged and do not change if we reduce  $\lambda/\Delta$  by an order of magnitude. The positivity constraint enabled the constrained minimisation problem to remain well posed in the limit of large (complete) orbital and auxiliary basis sets. Consequently, we expect the screening charge to change gradually, as we increase the size of the auxiliary basis. This effect will be stronger for systems with few electrons, since then, the difference between  $N - 1$  and  $N$  is largest.

Calculations were performed in the Gaussian basis set code HIPPO[30], with one- and two-electron integrals for the Cartesian Gaussian basis elements calculated using the GAMESS code [31, 33]. Basis set data was obtained from the Basis Set Exchange database [32].

In Figs. 1a-1c, the CLDA xc potential is shown for the Ne atom and three auxiliary basis sets, un-contracted cc-pVXZ, with X=D,T,Q. In each sub-figure  $v_{xc}^{CLDA}(r)$  is shown for fixed auxiliary basis and various orbital basis sets: cc-pVXZ [30, 34], with X=D,T,Q,5. For comparison, the LDA potential  $v_{xc}^{LDA}(r)$  is also shown with a blue dashed line.

In Figs. 2a-2c,  $r^2\rho_{scr}(r)$  (CLDA screening density multiplied by  $r^2$ ), is shown for the Ne atom and three auxiliary basis sets, un-contracted cc-pVXZ [30, 34], with X=D,T,Q. In each sub-figure  $r^2\rho_{scr}(r)$  is shown for fixed auxiliary basis and various orbital basis sets: cc-pVXZ [30, 34], with X=D,T,Q,5. The overall convergence of the xc potential is excellent. The

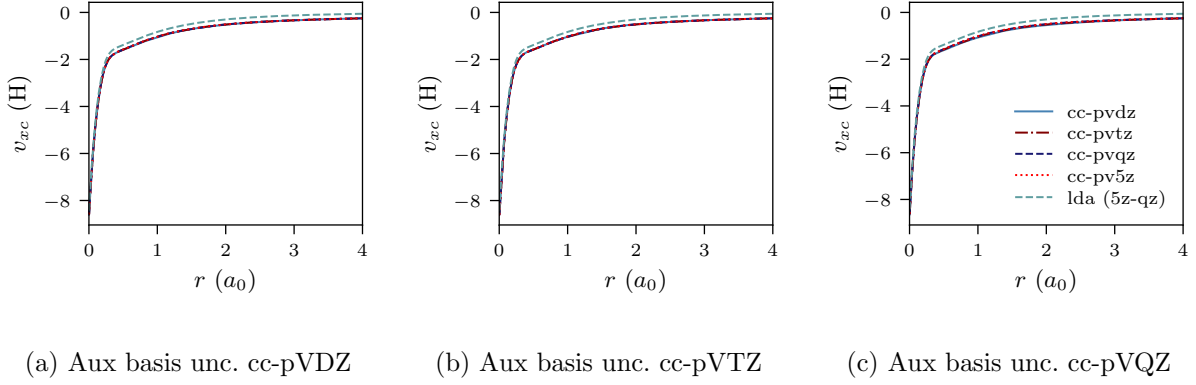


FIG. 1: Ne atom, CLDA xc potentials  $v_{xc}(r)$  using fixed auxiliary basis sets with various orbital basis sets. Blue dashed line is LDA.

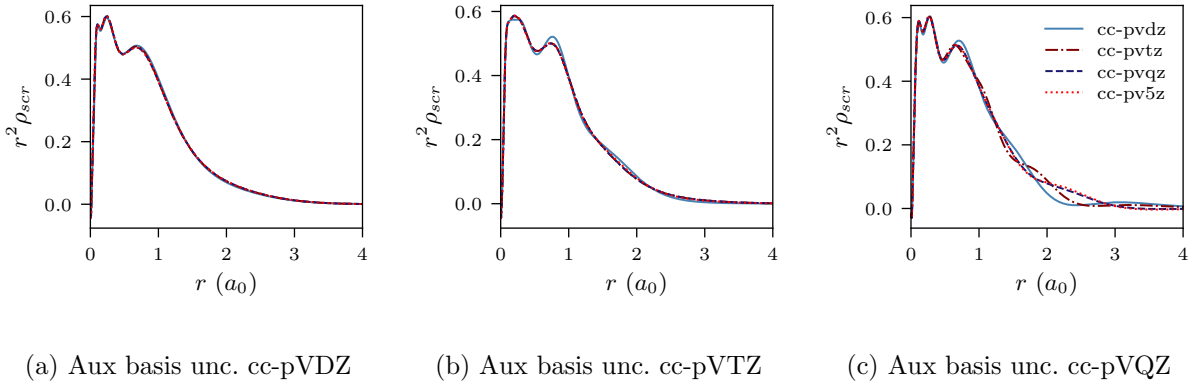


FIG. 2: Ne atom, CLDA results for  $r^2 \rho_{scr}(\mathbf{r})$ . Fixed auxiliary basis set for the expansion of  $\rho_{scr}(r)$  in each subfigure, various orbital basis sets.

convergence of  $\rho_{scr}(r)$  for fixed aux basis and increasing size of orbital basis is also very good. Before proceeding, it is worth pointing out that despite not deploying the positivity constraint (6) that would restrict the flexibility of the screening density and the xc potential, the latter (solutions of CLDA-OEP equations 12, 15 in Ref. 10) turn out to be smooth functions, not showing any wild oscillations characteristic of OEP-finite-basis pathologies, for any combination of orbital and auxiliary basis sets. This confirms our claim that by extending the domain of the density-density response function (7, 12), the solution of finite-basis-OEP equations is well behaved.

Figs. 3a-3c, 4a-4c show similar results to previous Figs. 1a-1c, 2a-2c, but for the Be atom.

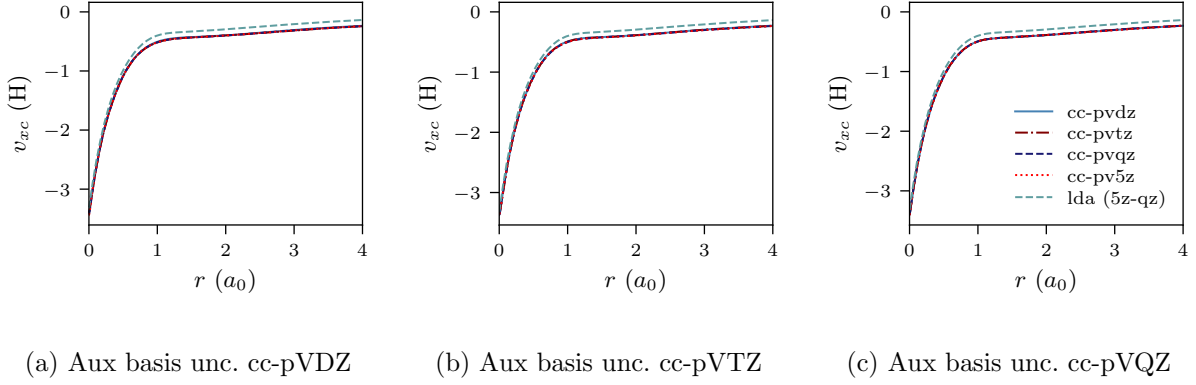


FIG. 3: Be atom, CLDA xc potentials  $v_{xc}(r)$  using fixed auxiliary basis sets with various orbital basis sets. Blue dashed line is LDA.

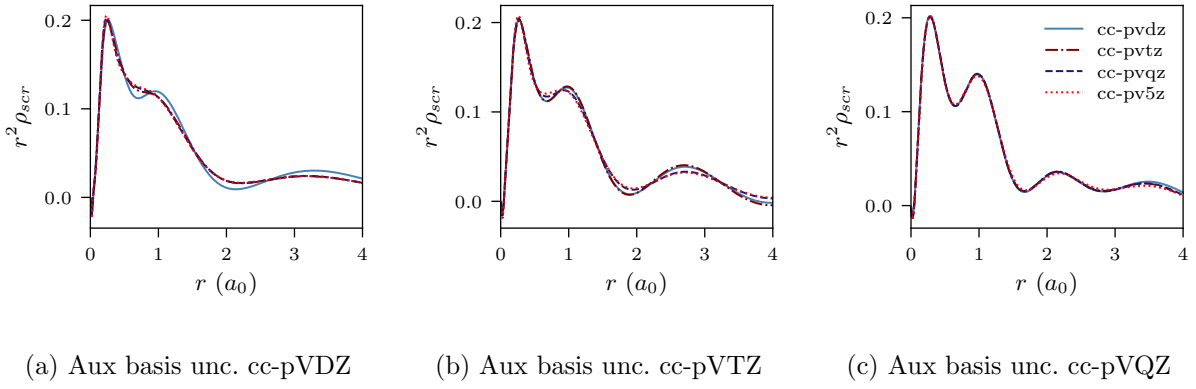


FIG. 4: Be atom, CLDA results for  $r^2 \rho_{scr}(\mathbf{r})$ . Fixed auxiliary basis set for the expansion of  $\rho_{scr}(r)$  in each subfigure, various orbital basis sets.

We proceed to discuss Figs. 5a-5c, 6a-6c, which show similar results as Figs. 1a-1c, 2a-2c, and 3a-3c, 4a-4c, for the He atom. The convergence of the xc potential *for fixed auxiliary basis* and increasing orbital basis size is good. Note that for any combination of orbital and auxiliary basis, the xc potential is smooth. The convergence of the screening density *for fixed auxiliary basis* and increasing size of orbital basis is slower than the other systems. In addition, as the size of the auxiliary basis increases, from 6a to 6b to 6c, the screening density keeps changing considerably. Note specifically the negative part of the screening density in Figs. 6a-6c. In Fig. 6a the negative lump is centred around  $2.5 a_0$  away from the origin, in Fig. 6b it is centred around  $3.0 a_0$  away from the origin and in Fig. 6c it has moved to  $3.5 a_0$ .



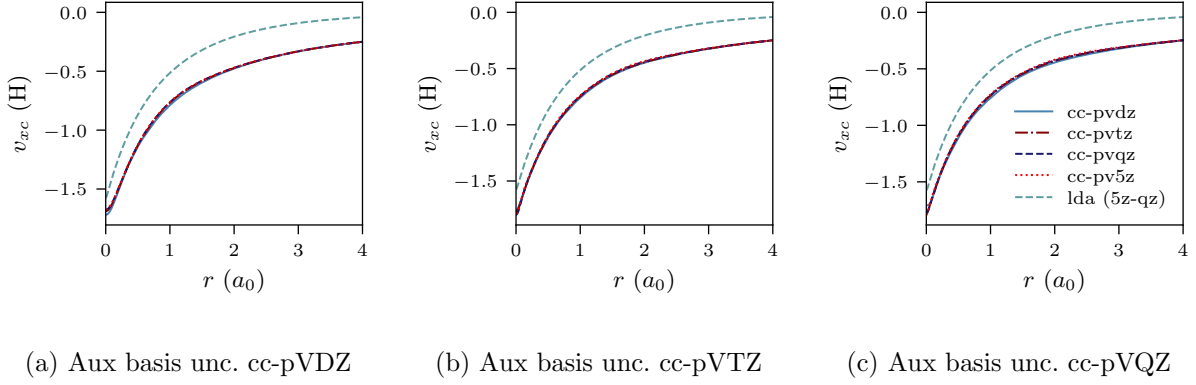


FIG. 5: He atom, CLDA xc potentials  $v_{xc}(r)$  using fixed auxiliary basis sets with various orbital basis sets. Blue dashed line is LDA.

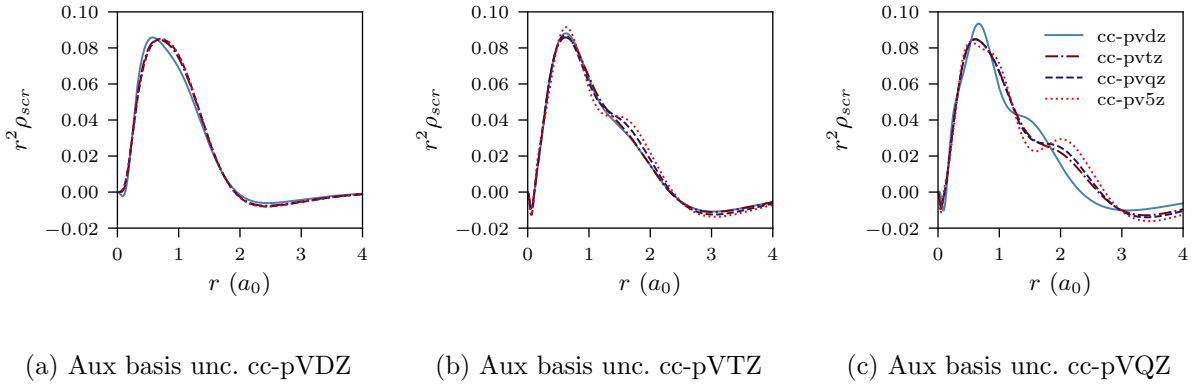


FIG. 6: He atom, CLDA screening densities  $\rho_{scr}(\mathbf{r})$  expanded in fixed auxiliary basis sets with various orbital basis sets.

This is the effect we discussed in section II. The positivity constraint enables the constrained minimisation problem to remain well posed for large basis sets (here large auxiliary bases). With only the constraint on  $Q_{scr}$  enabled and without positivity, it becomes energetically preferable, during the total energy minimisation, to converge to a screening density with the screening charge locally equal to  $N$  ( $=Q_{scr}^{LDA}$ ), and to shift negative charge density away from the system. The effect is already evident for the moderately large auxiliary bases used in our study, because the difference between  $N - 1$  and  $N$  is relatively large for  $N = 2$ .

The negatively charged ions is another class of difficult systems where LDA fails qualitatively. In Figs. 7a-7c, 8a-8c we plot the CLDA xc potential and screening density of

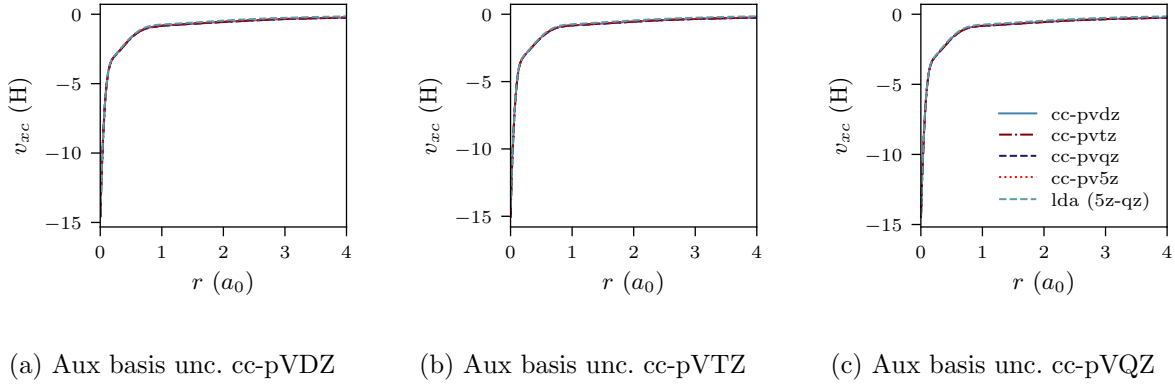


FIG. 7:  $\text{Cl}^-$  anion, CLDA xc potentials  $v_{xc}(r)$  using fixed auxiliary basis sets with various orbital basis sets (augmented). Blue dashed line is LDA. Convergence with increasing size of orbital basis is evident.

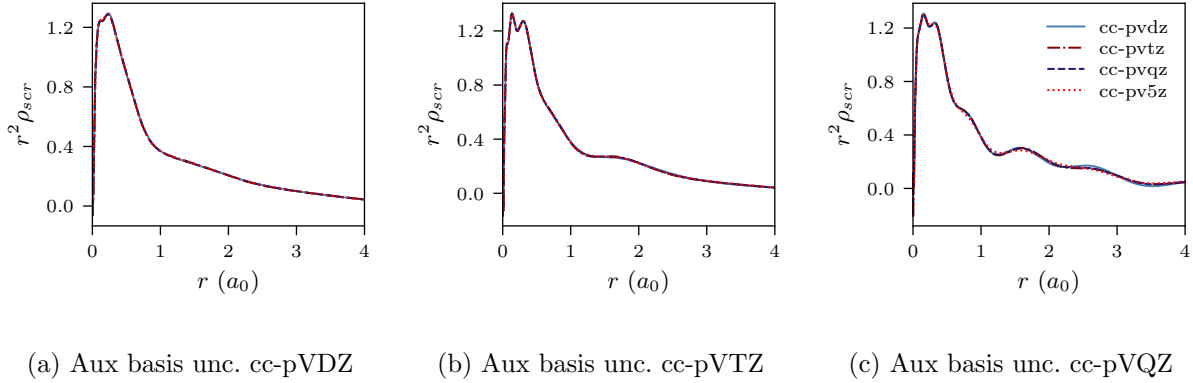


FIG. 8:  $\text{Cl}^-$  anion, CLDA screening densities  $\rho_{scr}(\mathbf{r})$  expanded in fixed auxiliary basis sets with various orbital basis sets. The screening density not converged.

the chlorine anion  $\text{Cl}^-$ . The orbital basis sets are augmented cc-pVXZ, with X=D,T,Q,5. It is evident that both the CLDA xc potential and the CLDA screening density are well converged and these systems do not present a challenge to the constrained minimisation, at least regarding convergence.

In Table I we show the IPs of several systems, including anions, obtained as the negative of the HOMO eigenvalue. For comparison with our previous CLDA method, in which we had imposed the positivity constraint, we show the CLDA IPs with (fourth column) and without positivity (fifth column). The results with positivity are from Ref. 8. The resulting

IPs do not depend strongly on the positivity constraint, except in helium, where we see a larger difference. We still see the familiar improvement of CLDA over the LDA results.

	Basis	LDA	CLDA pos	CLDA no pos	Exp
He	T-Q	15.46	23.14	21.57	24.6
Be	T-T	5.59	8.62	8.11	9.32
Ne	T-T	13.16	18.94	18.94	21.6
H <sub>2</sub> O	T-T	6.96	11.24	11.34	12.8
NH <sub>3</sub>	T-T	6.00	9.81	9.77	10.8
CH <sub>4</sub>	D-D	9.28	12.52	10.51	14.4
C <sub>2</sub> H <sub>2</sub>	D-D	7.02	10.63	10.31	11.5
C <sub>2</sub> H <sub>4</sub>	D-D	6.67	9.57	9.35	10.7
CO	D-D	8.75	12.73	12.11	14.1
NaCl	D-D	5.13	7.87	7.82	8.93
F <sup>-</sup>	T <sup>a</sup> -T	$\epsilon_H > 0$	2.23	2.16	3.34
Cl <sup>-</sup>	T <sup>a</sup> -T	$\epsilon_H > 0$	2.61	2.59	3.61
OH <sup>-</sup>	T <sup>a</sup> -T	$\epsilon_H > 0$	0.99	0.93	1.83
CN <sup>-</sup>	T <sup>a</sup> -T	0.13	2.87	2.86	3.77

TABLE I: The IPs of selected atoms, molecules (top) and negative ions (bottom) are shown in columns 3-5. The IPs are obtained as the negative of the HOMO eigenvalue  $\epsilon_H$  of the neutral system or the anion. The positivity constraint is employed for the results in column 4 (from Ref. 8) and relaxed for the results in column 5. The experimental IPs and electron affinities are shown in the sixth column. In the second column, X-Y stands for basis sets cc-pVXZ [30, 34] and uncontracted cc-pVYZ for the expansion of orbitals and screening charge densities. All energies are in eV.

<sup>a</sup>For the negative ions, the orbital basis was aug-cc-pVTZ.

In concluding this section, we note that for the auxiliary basis sets we tested, it is safe to carry out constrained minimisations of the DFA total energy under the constraint of the screening charge only,  $Q_{scr} = N - 1$ , except for systems with few electrons, where the omission of the positivity constraint manifests itself in shifting negative screening density

away from the origin.

In the next section, we shall argue that the screening charge constraint endows the xc potential of local and semi-local DFAs with exotic qualities, such a finite derivative discontinuity  $\Delta_{xc}$ . Although crucial for the accurate prediction of band gaps,  $\Delta_{xc}$  is notoriously hard to capture in approximations. (See however Ref. 29)

### III. DERIVATIVE DISCONTINUITY OF THE CDFA XC POTENTIAL

The discontinuity of the xc potential is defined by

$$\Delta_{xc} = \lim_{\omega \rightarrow 0^+} \Delta_{xc}^{\omega}(\mathbf{r}), \quad \text{with } \Delta_{xc}^{\omega}(\mathbf{r}) = v_{xc}^{N+\omega}(\mathbf{r}) - v_{xc}^{N-\omega}(\mathbf{r}) \quad (13)$$

where  $v_{xc}^{N\pm\omega}(\mathbf{r})$  is the xc potential of an ensemble with  $N \pm \omega$  electrons.

The ensemble KS densities with  $N \pm \omega$  electrons are given by,

$$\rho_{ven}^{N-\omega}(\mathbf{r}) = \omega \rho_{ven}^{N-1}(\mathbf{r}) + (1 - \omega) \rho_{ven}^N(\mathbf{r}), \quad (14)$$

$$\rho_{ven}^{N+\omega}(\mathbf{r}) = (1 - \omega) \rho_{ven}^N(\mathbf{r}) + \omega \rho_{ven}^{N+1}(\mathbf{r}), \quad (15)$$

where  $\rho_{ven}^M(\mathbf{r})$ ,  $M = N - 1, N, N + 1$ , is the ground state density of the  $M$ -electron KS system in the external potential  $v_{en}(\mathbf{r})$ .

We seek the derivative discontinuity  $\Delta_{xc}$  of the CLDA xc potential from (13) for reference. In order to obtain  $\Delta_{xc}^{\omega}(\mathbf{r})$  and then  $\Delta_{xc}$ , one must first find the ensemble KS xc potentials with densities  $\rho_{ven}^{N\pm\omega}(\mathbf{r})$  and subtract them. Work is in progress in our group to obtain directly these ensemble KS xc potentials. Here, we use an elegant method by Kraisler, Hodgson and Gross [25] to obtain the ensemble KS xc potential by constructing the ensemble density  $\rho_{ven}^{N\pm\omega}$  from separate KS calculations for  $N$ , and  $N \pm 1$  particles and then inverting  $\rho_{ven}^{N\pm\omega}(\mathbf{r})$  to obtain  $v_{xc}^{N\pm\omega}(\mathbf{r})$ .

Let us follow this construction in detail. The two KS ground state densities that build the ensemble density  $\rho_{ven}^{N+\omega}(\mathbf{r})$  can be written:

$$\rho_{ven}^N(\mathbf{r}) = \sum_{i=1}^N |\phi_i[\rho^N](\mathbf{r})|^2 \quad (16)$$

$$\rho_{ven}^{N+1}(\mathbf{r}) = \sum_{i=1}^{N+1} |\phi_i[\rho^{N+1}](\mathbf{r})|^2 \quad (17)$$

The notation makes explicit that  $\{\phi_i[\rho^M](\mathbf{r})\}$  are the KS orbitals of the  $M$ -electron system with density  $\rho^M$ .

The ensemble density then is:

$$\rho_{v_{en}}^{N+\omega}(\mathbf{r}) = \frac{1}{2} \sum_{i=1}^N \left[ |\phi_i[\rho^N](\mathbf{r})|^2 + |\phi_i[\rho^{N+1}](\mathbf{r})|^2 \right] + \omega |\phi_{N+1}[\rho^{N+1}](\mathbf{r})|^2 \quad (18)$$

In general, the ensemble KS orbitals,  $\{\phi_i[\rho^{N+\omega}](\mathbf{r})\}$ , will be linear combinations of the two sets of KS orbitals. However, in the asymptotic region the picture is very simple. For any  $\omega > 0$ , the density  $|\phi_{N+1}[\rho^{N+1}](\mathbf{r})|^2$  of the  $N + 1$  orbital will be the dominant term as every other term in the ensemble density will have died out. Hence the tail of the  $(N + 1)$ -th ensemble-KS orbital,  $\phi_{N+1}[\rho^{N+\omega}](\mathbf{r})$ , will be equal, within a phase, to the tail of  $\phi_{N+1}[\rho^{N+1}](\mathbf{r})$ . However,  $\phi_{N+1}[\rho^{N+1}](\mathbf{r})$  is a KS orbital of the  $N + 1$  electron system and in the asymptotic region it feels the net Coulomb repulsion of a screening charge of  $N$  electrons. Consequently,  $\phi_{N+1}[\rho^{N+\omega}](\mathbf{r})$ , in the asymptotic region, must feel the Coulomb repulsion of an equal amount of screening charge. Since the ensemble-KS orbitals lie in a common KS potential, the screening charge of the ensemble-screening-density will be  $Q_{scr}^{N+\omega} = N$ , for any finite  $\omega > 0$ .

We conclude that when the number of electrons increases past an integer value, the value of the screening charge  $Q_{scr}^{N+\omega}$  increases stepwise,

$$Q_{scr}^{M+\omega} = M, \text{ with } M = N, N \pm 1, \dots \text{ and } 0 < \omega \leq 1. \quad (19)$$

In the limit  $\omega \rightarrow 0^+$ , we have:

$$Q_{scr}^N = N - 1, \quad Q_{scr}^{N+} = N, \quad (20)$$

where  $Q_{scr}^{N+} = \lim_{\omega \rightarrow 0^+} Q_{scr}^{N+\omega}$ .

This stepwise increase of screening charge obviously causes a discontinuous jump in the constrained xc potential  $v_{xc}^{N+\omega}(\mathbf{r})$ . In the limit  $\omega \rightarrow 0^+$ , the jump of the xc potential is  $v_{xc}^{N+}(\mathbf{r}) - v_{xc}^N(\mathbf{r})$ , where  $v_{xc}^{N+}(\mathbf{r}) = \lim_{\omega \rightarrow 0^+} v_{scr}^{N+\omega}(\mathbf{r})$ . From (13) the jump of the xc potential due to the stepwise increase in the screening charge gives the derivative discontinuity in the CDFA method,

$$\Delta_{xc}^{CDFA} = v_{xc}^{N+}(\mathbf{r}) - v_{xc}^N(\mathbf{r}). \quad (21)$$

We note that Eq. 21 does not require an ensemble calculation, but only the evaluation of the  $N$ -electron CDFA xc potential for two values of the screening charge.

In the last part of the paper, we shall compare  $\Delta_{xc}$  from the constrained minimisation method (21) with the result for  $\Delta_{xc}$  from (13). We shall calculate the differences

$$\Delta_{xc}^{\omega}(\mathbf{r}) \simeq v_{xc}^{N+\omega}(\mathbf{r}) - v_{xc}^N(\mathbf{r}) \quad (22)$$

in CLDA for various values of  $\omega$  and investigate the limit of small  $\omega$ .

To construct the ensemble density  $\rho_{ven}^{N+\omega}(\mathbf{r})$  we need the densities from two KS calculations for  $N$  and  $N + 1$  particles. We use our CLDA method to obtain the densities  $\rho_{ven}^N(\mathbf{r})$  and  $\rho_{ven}^{N+1}(\mathbf{r})$ , in order to control the screening densities of the constituent xc potentials. One of the integers  $N$ ,  $N + 1$  is an odd number, corresponding to an open shell system. The LDA exchange energy for open shells contains an error (“ghost-exchange error” [26]) in modelling exchange with half the electrons spin-up and half spin-down. In a forthcoming publication[26], we propose how to correct this error, still within LDA (not local spin density approximation). Hence, in the KS calculation for an odd number of electrons (either for  $N$  or for  $N + 1$ ), we employ our method to correct for the ghost-exchange error, in order to improve the accuracy of the resulting CLDA xc potential and density. Details will be published in Ref. 26.

Once we construct the ensemble density, we invert it to obtain the ensemble KS potential,  $v_{xc}^{N+\omega}(\mathbf{r})$ . For the inversion, we apply the method in Refs. 27, 28. The inversion method [27] requires the selection a priori of the screening charge of the xc potential. According to (19), for  $v_{xc}^{N+\omega}(\mathbf{r})$  we set  $Q_{scr}^{N+\omega} = N$ .

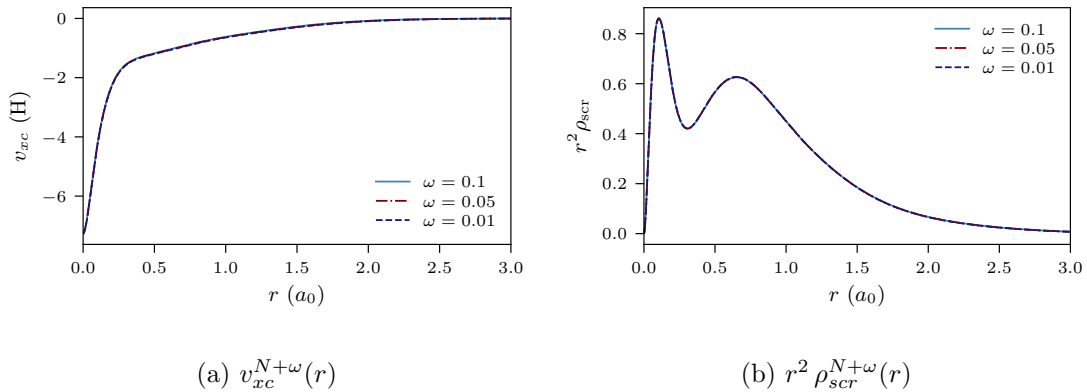
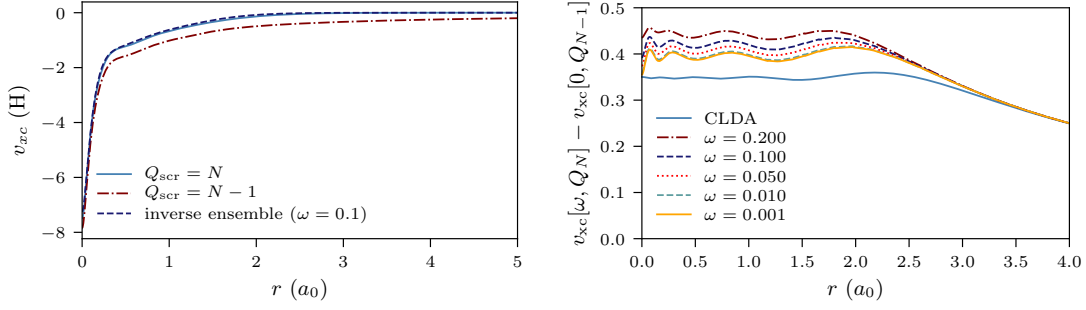


FIG. 9: Ne atom, ensemble xc potentials and screening densities for various values of  $\omega$ .

The orbital and auxiliary basis sets are uncontracted cc-pVTZ.



(a) xc potentials  $v_{xc}^{N+\omega}(r)$  and  $v_{xc}^N(r)$ ,  $v_{xc}^{N+}(r)$ . (b)  $\Delta_{xc}^\omega(r)$  for various  $\omega$ . Blue line is  $\Delta_{xc}^{CLDA}$ .

FIG. 10: Ne atom, xc potentials and differences of xc potentials. The orbital and auxiliary basis sets are uncontracted cc-pVTz.

In Figs. 9a, 9b the ensemble xc potentials,  $v_{xc}^{N+\omega}(r)$  and screening densities are shown, for various values of  $\omega$ , obtained by inverting the ensemble densities (18). The screening charge for the ensemble densities is set  $Q_{scr}^{N+\omega} = N$ . The xc potentials and screening densities are very close, as expected, which is an indication of the quality of convergence and the inversion method.

In Fig. 10a, the ensemble xc potential,  $v_{xc}^{N+\omega}(r)$ , for  $\omega = 0.1$  (with  $Q_{scr}^{N+\omega} = N$ ) is shown together with  $v_{xc}^N(r)$  and  $v_{xc}^{N+}(r)$ , which have screening charges  $Q_{scr}^N = N - 1$  and  $Q_{scr}^{N+} = N$ .

In Fig. 10b, the  $\omega$ -dependent (22) derivative discontinuity,  $\Delta_{xc}^\omega(r) = v_{xc}^{N+\omega}(r) - v_{xc}^N(r)$ , is shown for various values of  $\omega$ . In the limit of small  $\omega$ ,  $\Delta_{xc}^\omega(r)$  yields the derivative discontinuity using ensembles,  $\Delta_{xc}^{\omega \rightarrow 0}(r) = \Delta_{xc}$ .

The blue line in Fig. 10b shows the CLDA prediction for the derivative discontinuity,  $\Delta_{xc}^{CLDA}$ , without an ensemble calculation.  $\Delta_{xc}^{CLDA}$  remains almost a constant up to a distance of about  $2.5 a_0$ . The differences  $\Delta_{xc}^\omega(r)$  for decreasing  $\omega$  approach the line of  $\Delta_{xc}^{CLDA}$  both in height and in the spatial extent over which  $\Delta_{xc}^{CLDA}$  and  $\Delta_{xc}^\omega$  stay almost constant.

#### IV. CONCLUSIONS

A common theme of popular local and semi-local density functional approximations is the imbalance of accuracy between energy density-functionals, which can be quite accurate, and the corresponding effective KS potentials, with inferior accuracy [1–3]. We have approached this problem from several directions [4, 7, 28]. In this paper, we review and expand our

work on imposing physical constraints during the energy minimisation [8–10]. Specifically, we investigate the relaxation of a constraint that is computationally expensive and find that its omission leads to well behaved results, except for very small systems with only a few electrons. The constraints we impose raise the total energy minimally [8, 10] but have a dramatic impact on the quality of the effective KS potential, gifting it with the correct asymptotic behaviour and enabling it to exhibit important non-analytic behaviour (derivative discontinuity) shared by the exact KS potential but elusive from the lower rungs of Jacob’s ladder of DFAs where semi-local DFAs reside.

### Acknowledgments

NIG and TP acknowledge financial support by The Leverhulme Trust, through a Research Project Grant with number RPG-2016-005.

NIG thanks Prof. Rod Bartlett for very helpful discussions during his visit at Durham University in early 2019 and acknowledge the Institute of Advanced Study at Durham University for hosting this visit.

- 
- [1] Bartlett, Rodney J. “Adventures in DFT by a wavefunction theorist.” *The Journal of chemical physics* 151, no. 16 (2019): 160901.
  - [2] Adam Wasserman, Jonathan Nafziger, Kaili Jiang, Min-Cheol Kim, Eunji Sim, Kieron Burke, *Annu. Rev. Phys. Chem.* **68**, 555–81 (2017)
  - [3] Eunji Sim, Suhwan Song, Kieron Burke, *J. Phys. Chem. Lett.*, **9**, 6385 (2018)
  - [4] N.I. Gidopoulos, “Progress at the interface of wave-function and density-functional theories”, *Phys. Rev. A* 83, 040502(R) (2011); DOI: 10.1103/PhysRevA.83.040502
  - [5] Irons, Tom JP, James W. Furness, Matthew S. Ryley, Jan Zemen, Trygve Helgaker, and Andrew M. Teale. “Connections between variation principles at the interface of wave-function and density-functional theories.” *The Journal of chemical physics*, **147**, 134107 (2017)
  - [6] T.W. Hollins, S.J. Clark, K. Refson, N.I. Gidopoulos, “A local Fock-exchange potential in Kohn–Sham equations”, *J. Phys.: Condens. Matter* 29 , 04LT01 (2017); doi:10.1088/1361-648X/29/4/04LT01



- [7] T. Callow, N.I. Gidopoulos, “Optimal power series expansions of the Kohn–Sham potential”, Eur. Phys. J. B, 91: 209 (2018); [https://doi.org/10.1140/ep\\_jb/e2018-90189-2](https://doi.org/10.1140/ep_jb/e2018-90189-2)
- [8] N.I. Gidopoulos, N.N. Lathiotakis, “Constraining density functional approximations to yield self-interaction free potentials”, J. Chem. Phys. 136, 224109 (2012); doi: 10.1063/1.4728156
- [9] N. Gidopoulos, N.N.Lathiotakis, “Chapter Six - Constrained Local Potentials for Self-Interaction Correction” Advances In Atomic, Molecular, and Optical Physics, Volume 64, Pages 129-142, (2015); <https://doi.org/10.1016/bs.aamop.2015.06.003>
- [10] T. Pitts, N.I. Gidopoulos, N.N. Lathiotakis, “Performance of the constrained minimization of the total energy in density functional approximations: the electron repulsion density and potential”, Eur. Phys. J. B 91: 130 (2018); [https://doi.org/10.1140/ep\\_jb/e2018-90123-8](https://doi.org/10.1140/ep_jb/e2018-90123-8)
- [11] T. Pitts, T. Callow, B. Pearce, NN Lathiotakis, NI Gidopoulos, to appear.
- [12] J.P. Perdew, K. Schmidt, AIP Conference Proceedings **577**, 1 (2001); <https://doi.org/10.1063/1.1390175>
- [13] R. T. Sharp and G. K. Horton, Phys. Rev. 90, 317 (1953).
- [14] J. D. Talman and W. F. Shadwick, Phys. Rev. A 14, 36 (1976).
- [15] A. Görling, PRL, **83**, 5459 (1999)
- [16] S. Liu, P. W. Ayers, and R. G. Parr, J. Chem. Phys. **111**, 6197 (1999).
- [17] P.W. Ayers, M. Levy, J Chem Phys, **115**, 4438 (2001); doi:10.1063/1.1379333
- [18] R. Bartlett, private communication.
- [19] V. N. Staroverov, G. E. Scuseria, and E. R. Davidson, J. Chem. Phys. 124, 141103 (2006); <https://doi.org/10.1063/1.2194546>
- [20] N.I. Gidopoulos, N.N. Lathiotakis, Phys. Rev. A 85, 052508 (2012); <https://doi.org/10.1103/PhysRevA.85.052508>
- [21] C. Friedrich, M. Betzinger, S. Blügel, Phys. Rev. A 88, 046501 (2013); <https://doi.org/10.1103/PhysRevA.88.046501>
- [22] N.I. Gidopoulos, N.N. Lathiotakis, Phys. Rev. A 88, 046502; <https://doi.org/10.1103/PhysRevA.88.046502>
- [23] A. Unsöld, Z. Phys. **43**, 563 (1927); <https://doi.org/10.1007/BF01397633>
- [24] T. Pitts, S. Bousiadi, N.I. Gidopoulos, N.N. Lathiotakis, to appear.
- [25] Eli Kraisler, M. J. P. Hodgson and E. K. U. Gross, to appear.
- [26] T.J. Callow, B. Pearce, N.I. Gidopoulos, to appear.

- [27] T.J. Callow, N.N. Lathiotakis, N.I. Gidopoulos, *J. Chem. Phys.* **152**, 164114 (2020); <https://doi.org/10.1063/5.0005781>
- [28] T.W. Hollins, S.J. Clark, K. Refson, N.I. Gidopoulos, *J. Phys.: Condens. Matter* **29**, 04LT01 (2017); doi:10.1088/1361-648X/29/4/04LT01
- [29] X. Andrade, A. Aspuru-Guzik, *Phys Rev Lett*, **107**, 183002 (2011); 10.1103/PhysRevLett.107.183002
- [30] Thom H. Dunning. Gaussian basis sets for use in correlated molecular calculations. I. The atoms boron through neon and hydrogen. *The Journal of Chemical Physics*, 90(2):1007–1023, 1989.
- [31] Mark S. Gordon and Michael W. Schmidt. Chapter 41 - advances in electronic structure theory: Gamess a decade later. In Clifford E. Dykstra, Gernot Frenking, Kwang S. Kim, and Gustavo E. Scuseria, editors, *Theory and Applications of Computational Chemistry*, pages 1167 – 1189. Elsevier, Amsterdam, 2005.
- [32] Benjamin P. Pritchard, Doaa Altarawy, Brett Didier, Tara D. Gibson, and Theresa L. Windus. New basis set exchange: An open, up-to-date resource for the molecular sciences community. *Journal of Chemical Information and Modeling*, 59(11):4814–4820, 2019. PMID: 31600445.
- [33] Michael W. Schmidt, Kim K. Baldridge, Jerry A. Boatz, Steven T. Elbert, Mark S. Gordon, Jan H. Jensen, Shiro Koseki, Nikita Matsunaga, Kiet A. Nguyen, Shujun Su, Theresa L. Windus, Michel Dupuis, and John A. Montgomery Jr. General atomic and molecular electronic structure system. *J. Comput. Chem.*, 14(11):1347–1363, 1993.
- [34] David E. Woon and Thom H. Dunning. Gaussian basis sets for use in correlated molecular calculations. III. The atoms aluminum through argon. *The Journal of Chemical Physics*, 98(2):1358–1371, 1993.
- [35] Calculated as the negative of the HOMO eigenvalue.